DOI 10.1007/s11595-014-1071-8

Influence of Mineral Admixtures on the Electro-deposition Healing Effect of Concrete Cracks

CHU Hongqiang[1], JIANG Linhua[1], YOU Lushen[1], XU Ning[1,2], SONG Zijian[1], ZHANG Yan[1]

(1.College of Mechanics and Materials, Hohai University, Nanjing 210098, China; 2.Nanjing Hydraulic Research Institute, Nanjing 210098, China)

Abstract: Two types of solutions ($ZnSO_4$, $MgSO_4$) were selected to study the influence of mineral admixtures on the electro-deposition healing effect of concrete cracks. Four parameters (*i e*, rates of weight gain, surface coating, crack closure and crack filling depth) were measured. The mineral composition of electro-deposits in the cracks was analyzed. The study shows that the healing effect of mortar specimens with 10% fly ash is the worst, while the healing effect of mortar specimens with 20% fly ash is better than that of the specimens without fly ash. The rates of weight gain, surface coating, crack closure and crack filling depth decrease with increasing content of the ground granulated blast-furnace slag(GGBS). The mineral admixtures have no influence on the composition of deposits.

Key words: electro-deposition; crack repair; mineral admixtures; healing effect

1 Introduction

The electro-deposition method is a new technique used to repair the cracks of reinforced concrete structure, which was first studied in Japan in late 1980s and makes full use of reinforced concrete characteristics and water environmental conditions, applies certain weak current to generate electrolytic deposition, grows and precipitates a layer of compounds (such as $Mg(OH)_2$, $CaCO_3$, *etc*) in the concrete cracks and on the concrete surface so as to heal the concrete cracks and close the concrete surface. According to this mechanism, researchers in Japan and USA conducted preliminary study on the applicability of electro-deposition method in repairing land concrete cracks and on the performance of shrinkage cracked concrete after electro-deposition rehabilitation in recent years[1-3]. However, the study on this technique in China has just started[4].

The mineral admixture is the sixth component of high performance concrete. The common admixtures contain fly ash and GGBS. The influence of fly ash and GGBS on the electro-deposition healing effect is rarely reported. In this paper, the influence of mineral admixtures and their percentage on the electro-deposition effect was presented.

2 Experimental

2.1 Raw materials

Table 1 Physical properties of cement

Cement type	Stability	Flexural strength /MPa		Compressive strength /MPa	
		3 d	28 d	3 d	28 d
P·Ⅱ42.5	Qualified	5.2	8.3	25.0	47.8

Table 2 Chemical composition of cement/wt%

SiO_2	Al_2O_3	Fe_2O_3	CaO	MgO	SO_3
21.52	5.13	5.25	63.86	1.46	2.28

P•II 42.5 cement produced by Chinese Cement Plant was used. The physical properties and chemical composition of the cement are shown in Tables 1 and 2, respectively. Fine aggregate was the natural river sand obtained from local sources. The physical properties of

(Received: Jan. 8, 2014; Accepted: Mar. 8, 2014)

CHU Hongqiang(储洪强): Ph D; E-mail: chq782009@126.com

Funded by the National Natural Science Foundation of China (Nos. 51479051, 51278167), the Natural Science Foundation of Jiangsu Province (No. BK20131374), and the Research and Innovation Project for College Graduates of Jiangsu Province (No. CXZZ12_0238)

river sand is shown in Table 3. The mineral admixtures were also obtained from local sources. The physical properties and chemical composition of fly ash are shown in Tables 4 and 5, respectively. The physical properties and chemical composition of GGBS are shown in Tables 6 and 7, respectively.

Table 3 Physical properties of fine aggregate

Apparent density /(kg/m^3)	Bulk density /(kg/m^3)	Mud content /%	Clod content /%	Fineness modulus	Grading zone
2 620	1 490	0.9	0.0	2.6	Ⅱ

Table 4 Physical properties of fly ash

Moisture content /%	45 μm screen residue/%	Water demand ratio/%	Activity index/%	
			7 d	28 d
0.1	8.2	90	90	95

Table 5 Chemical composition of fly ash/wt%

SiO_2	Al_2O_3	Fe_2O_3	TiO_2	CaO	MgO	SO_3	LOI
50.32	33.6	4.00	1.32	0.9	5.16	0.41	1.20

Table 6 Physical properties of GGBS

Moisture content /%	Specific surface area /(m^2/kg)	Water demand ratio/%	Activity index/%		
			3 d	7 d	28 d
0.1	410	95	85	90	98

Table 7 Chemical composition of GGBS/wt%

SiO_2	Al_2O_3	Fe_2O_3	CaO	MgO	TiO_2	MnO	SO_3	LOI
32.08	15.6	0.86	36.93	10.15	0.82	0.45	0.91	0.40

2.2 Specimen preparation

Reinforced mortar prism specimens, with dimensions of 40 mm×40 mm×160 mm were prepared for the following investigation. The cover depth of these specimens was 1.5 cm. The water-cement ratio of concrete specimens was 0.60 and the cement-sand ratio was 1:2.5. The diameter of the plain steel bar was 6 mm. After curing the specimens under standard conditions for 28 days, the load-induced cracks of 0.3 mm ± 0.05 mm in width on the mortar surface were made in all specimens, which were used to simulate the flexural cracks in practical engineering. Except for the cracked side, all of the other five sides of each specimen were sealed with silicone rubber. Finally, the specimens were placed in a tank containing electrolyte solution.

2.3 Experimental procedure

0.25 mol/L $ZnSO_4$ and 0.25 mol/L $MgSO_4$ electrolyte solutions were used in this study. The auxiliary electrode was a flake titanium mesh with electrode distance of 40 mm and the current density of 2.0 A/m^2. The fly ash and GGBS were mixed separately. The mixing content was 0%, 10% and 20%. Three specimens were prepared in each group, and totally 30 specimens were used in this experiment. In order to maintain the same concentration, the solutions were replaced every 5 days. The test lasted for 20 days.

3 Evaluation index of electro-deposition healing effect

The electrodeposition speed could be reflected by the weight gain. The effect of erosion resistance of concrete with cracks that improved by the electrodeposition treatment is closely related to sediment coverage, crack closure, and the filling of cracks by sediment[3,4]. Thus, the rates of weight gain, surface coating, crack closure as well as crack filling depth were used to evaluate the formation of electrodeposits in the concrete cracks.

3.1 Rate of weight gain

The specimens were taken out at an interval of 5 days. The samples were cured for 24 hours at 20±2 ℃ and 60±5% RH. Then the corresponding mass was weighed. The rate of weight gain could be calculated by:

$$R_m = \frac{M_i}{M} \times 100\% \quad (1)$$

where, R_m is the rate of weight gain (%), M_i is the weight gain (g), and M is the total weight before electro-deposition treatment (g).

3.2 Rate of surface coating

The rate of surface coating was measured from the beginning of the test. The specimens were taken out at an interval of 5 days. The photos were taken and the rate of surface coating could be calculated by:

$$R_a = \frac{A_c}{A} \times 100\% \quad (2)$$

where, R_a is the rate of surface coating (%), A_c is the coated surface area (mm^2), and A is the total area of the surface (mm^2).

3.3 Rate of crack closure

The rate of crack closure was measured from the beginning of the test. Eq.(3) is used to calculate the rate of crack closure of the mortar specimens:

$$R_l = \frac{L_c}{L} \times 100\% \quad (3)$$

where, R_1 is the rate of crack closure (%), L_c is the length of closed crack (mm), and L is the total length of crack (mm).

3.4 Crack filling depth

The crack filling depth was also measured from the beginning of the test. After electro-deposition, the mortar specimens with cracks were splitted laterally along the cracks. Ten locations at equal intervals were selected to measure the filling depths with Vernier Caliper. The crack filling depth is the average value of the ten measurements.

4 Results and discussion

After the circuit being connected, air bubbles came out immediately near the surface of the mortar specimens and the titanium mesh. Taking out the specimens every five days, white deposits were found on the surface and in the cracks of the specimens. The deposits increased with time. The experiments were finished in 20 days. The details of the surface and cracks of the mortar specimens after electro-deposition are shown in Fig.1 and Fig.2, respectively.

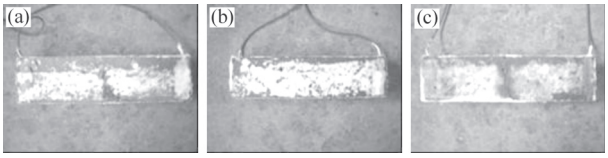

Fig.1 Details of the surface of specimens after electrodeposition

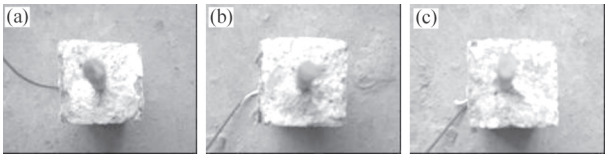

Fig. 2 Details of the cracks of specimens after electro-deposition

4.1 Analysis on the electro-deposition healing effect

4.1.1 Influence of fly ash on the electro-deposition healing effect

Fig.3 shows the variation of the rate of weight gain with different percentage of fly ash. Fig.4 shows the variation of the rate of surface coating. Fig.5 shows the variation of the rate of crack closure. Fig.6 demonstrates how the crack filling depth varies with the change of content of fly ash.

Results from Fig.3 to Fig.6 show the impact of fly ash on the electro-deposition healing effect. After charging for 20 days, the cracks of the specimens

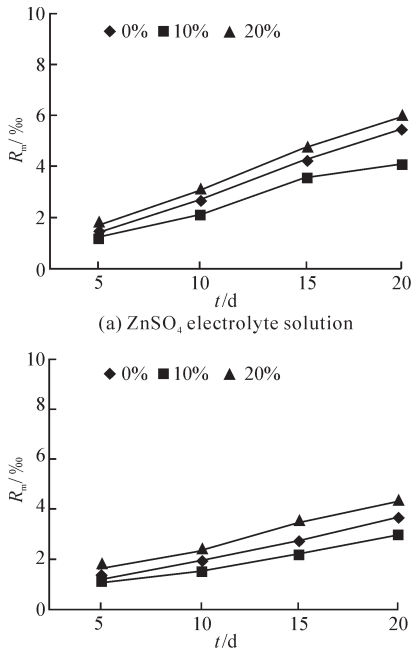

Fig.3 Rate of weight gain versus age with different percentages of fly ash

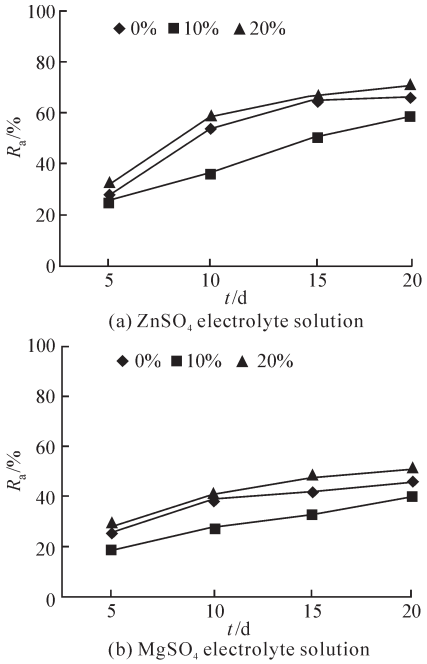

Fig.4 Rate of surface coating versus age with different percentages of fly ash

mixed with 20% fly ash are all closed (the rate of crack closure is 100%). When $ZnSO_4$ electrolyte solution was adopted, the range of the mass increasing rate was from 4.2‰ to 5.9‰.The rate of surface coating ranged from 58.6% to 70.5% and the crack filling depth lay between 5.6 mm and 9.1 mm. When $MgSO_4$ electrolyte solution was adopted, the range of the mass increasing rate was from 3.0‰ to 4.3‰. The rate of

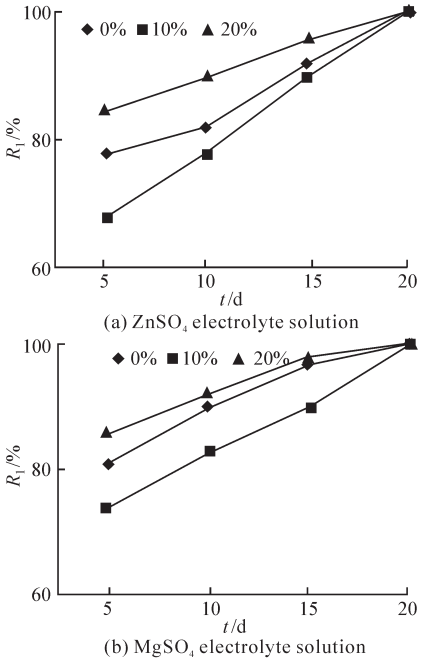

(a) $ZnSO_4$ electrolyte solution

(b) $MgSO_4$ electrolyte solution

Fig. 5 Rate of crack closure versus age with different percentages of fly ash

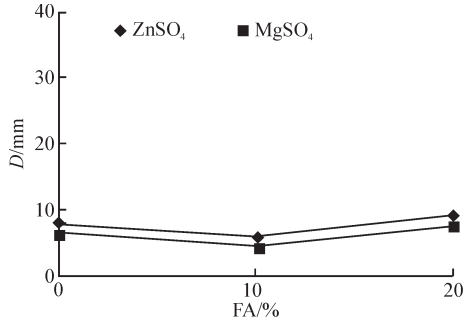

Fig.6 Crack filling depth versus content of fly ash

surface coating ranged from 39.6% to 51.2% and the crack filling depth lay between 4.2 mm and 7.3 mm. Among the three kinds of admixture content, the concrete specimens with 10% fly ash had the worst electro-deposition healing effect. The healing effect of concrete specimens mixed with 20% fly ash performed better than that of the specimens without fly ash. As we know, the chemical compositions of fly ash and cement were basically the same. However, the CaO content of fly ash is far lower than that of cement while the SiO_2 content is higher. Therefore, the CaO content in the raw materials is reduced after the fly ash is mixed. Moreover, the hydration products of fly ash and cement generate the "secondary hydration reaction" to reduce the production of $Ca(OH)_2$. The reduction of OH^- volume in the specimen reduced the probability that OH^- is separated out and combines with positive ion (Zn^{2+}, Mg^{2+}) to generate deposits. In addition, the secondary hydration function can be brought into full play in a medium or long term due to the lower activity of fly ash. Therefore, mixing 10% fly ash can improve the concentration of the concrete to a certain degree, which goes against the internal diffusion of ions such as Zn^{2+}, Mg^{2+} and OH^- in concrete. In that case, the resistance separating OH^- from mortar specimens is increased. Furthermore, the electric resistance of mortar specimens is improved to generate lower current inside them so as to reduce the passing electric charge quantity. Thus, the opportunity of deposit generation by ion combination inside the specimens and in the cracks is reduced. When mixed with 20% fly ash, the early density of concrete is reduced, but the opportunity of deposit generation by combining Zn^{2+}, Mg^{2+} and OH^- increased. At that time, this effect is dominating and greater than the negative influence brought by reduction of concrete specimen internal OH^-. Therefore, the deposition effect of concrete specimens mixed with 20% fly ash is slightly better than that of the specimens without fly ash.

4.1.2 Influence of GGBS on the electro-deposition healing effect

The rates of weight gain, surface coating, and crack closure of the specimens mixed with 0%, 10% and 20% GGBS in different charging times are shown in Figs.7-9, respectively. The relationship between the crack filling depth and the percentage of GGBS can be found in Fig.10.

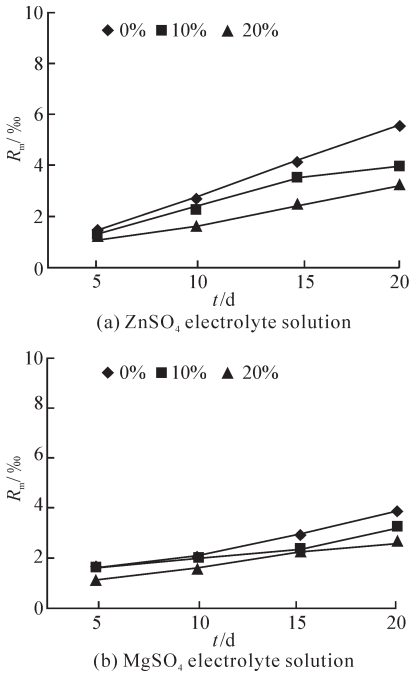

(a) $ZnSO_4$ electrolyte solution

(b) $MgSO_4$ electrolyte solution

Fig.7 Rate of weight gain versus age with different percentages of GGBS

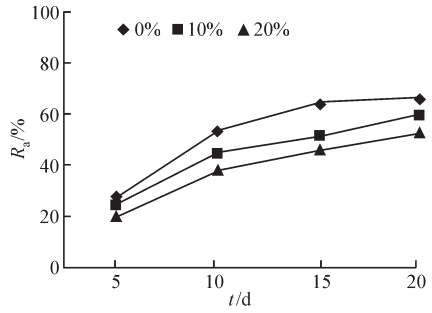

(a) $ZnSO_4$ electrolyte solution

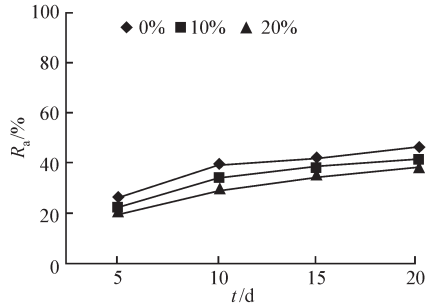

(b) $MgSO_4$ electrolyte solution

Fig.8 Rate of surface coating versus age with different percentages of GGBS

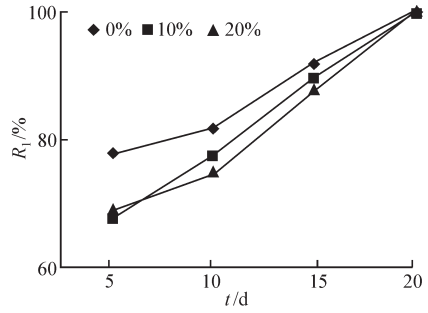

(a) $ZnSO_4$ electrolyte solution

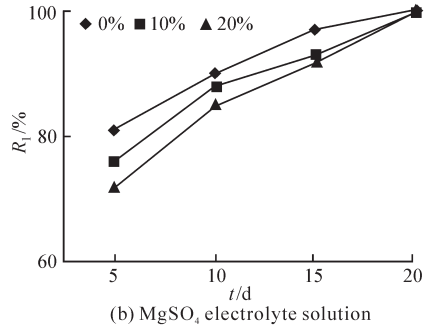

(b) $MgSO_4$ electrolyte solution

Fig.9 Rate of crack closure versus age with different percentages of GGBS

The results show that the cracks of the specimens mixed with 20% GGBS are all closed after charging for 20 days (the rate of crack closure is 100%). When $ZnSO_4$ solution is adopted, the specimens are with the mass increasing rate of max. 5.5‰ and min.3.3‰, the rate of surface coating ranged from 52.8% to 66.3% and the crack filling depth between 5.0 mm and 7.8 mm. When $MgSO_4$ solution is adopted, the specimens are with the mass increasing rate of max. 3.8‰ and min.2.6‰, the rate of surface coating ranged from 38.5% to 46.0% and the crack filling depth between 4.2 mm and 6.5 mm. Among the three kinds of admixture contents, all of the electro-deposition healing effect (the rates of weight gain, surface coating, crack closure and crack filling depth) becomes worse as the content increases. As we know, the chemical compositions of GGBS and cement are basically the same. However, the CaO content is far lower than that of cement and the SiO_2 content is higher. Therefore, the CaO content in the raw materials is reduced after the GGBS is mixed. Moreover, the hydration products of GGBS and cement generate the "secondary hydration reaction" to reduce the production of $Ca(OH)_2$ the hydration product. The reduction of OH^- volume in the specimen reduced the probability that OH^- is separated out and combines with positive ion (Zn^{2+}, Mg^{2+}) to generate deposits. In addition, because the GGBS is finer than the cement grains, the GGBS grains are filled in the gap between cement grains. After 28 days' standard maintenance, some mineral GGBS have participated in the "secondary hydration reaction" to form density filling structure and microscopic level close packing system[5] and to reduce the porosity of cement mortar. Therefore, the densities of concrete mixed with 10% and 20% GGBS are improved[6,7]. Moreover, when the content is 20%, the density is further improved. In that case, the electric resistance of mortar is increased so as to generate smaller current and reduce the passing electric charge quantity correspondingly. Furthermore, the resistance separating OH^- from mortar specimens increased so that the opportunity of deposit generation reduced. Therefore, the rates of weight gain, surface coating, crack closure and crack filling depth of specimens all reduce as the GGBS content increases.

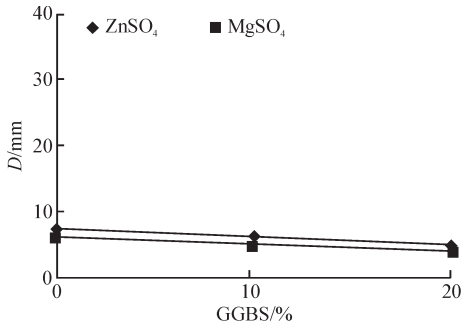

Fig. 10 Crack filling depth versus content of GGBS

4.2 Deposit composition analysis

XRD technique was used to analyze the deposits

in cracks of specimen mixed with 20% fly ash and GGBS. The corresponding XRD patterns are shown in Fig.11 and Fig.12 for fly ash mixture and GGBS mixture, respectively.

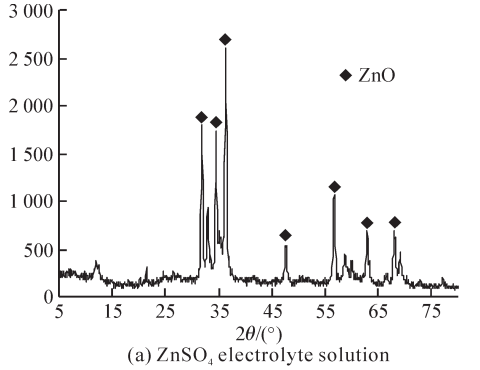

(a) $ZnSO_4$ electrolyte solution

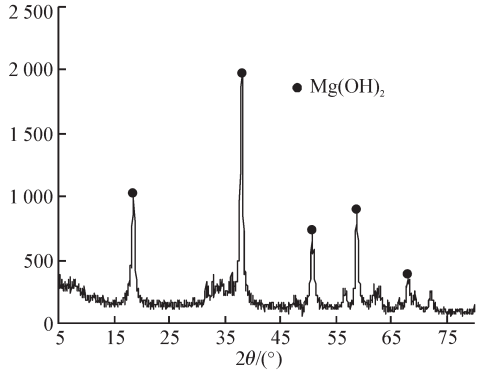

(b) $MgSO_4$ electrolyte solution

Fig.11 XRD patterns of deposits in the cracks of the specimen mixed with 20% fly ash

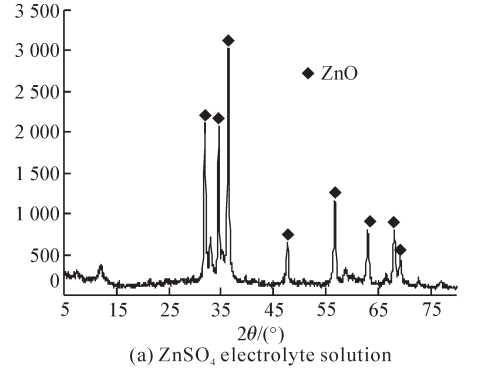

(a) $ZnSO_4$ electrolyte solution

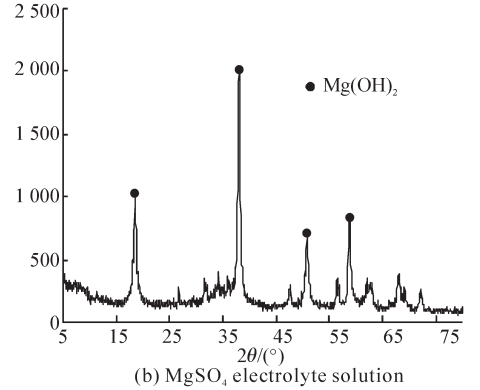

(b) $MgSO_4$ electrolyte solution

Fig.12 XRD patterns of deposits in the cracks of the specimen mixed with 20% GGBS

Comparing Figs.11(a) and 12(a) with JCPDS card, it`s found that the diffraction crystal plane of each pattern is consistent with the standard ZnO diffraction peak without other impurity peak, which indicates that the deposits in cracks are all ZnO with pure crystals. The narrow and sharp diffraction peak shape indicates that the crystallinity degree of deposits is high. As shown in Figs.11(b) and 12(b), the XRD patterns of deposits in cracks of the specimens mixed with 20% fly ash or 20% GGBS have sharp characteristic peaks, which show the favorable crystallinity of deposits. Through the comparison with JCPDS card, the diffraction peak positions of the specimens are consistent with the peak shape of standard $Mg(OH)_2$ pattern, which means that the crystal structure of $Mg(OH)_2$ is not affected after mixed with admixture. There is almost no other characteristic peak except the characteristic peak of $Mg(OH)_2$ in the XRD pattern, which shows the higher purity of $Mg(OH)_2$.

5 Conclusions

The influence of mineral admixtures on the electro-deposition healing effect was investigated using zinc salt and magnesium salt solutions. Four parameters (*i e*, rate of weight gain, surface coating, crack closure and crack filling depth) were measured. The mineral composition of electrodeposits in the cracks was analyzed. Results showed that the healing effect of mortar specimens with 10% fly ash was the worst. The healing effect of mortar specimens with 20% fly ash was better than that of the specimens without fly ash. The rates of weight gain, surface coating, crack closure and crack filling depth became worse as the GGBS percentage increased. The concrete admixtures have no influence on the composition of deposits.

References

[1] Otsuki N and Ryu JS. Use of Electrodeposition for Repair of Concrete with Shrinkage Cracks[J]. *Materials in Civil Engineering*, 2001, 13(2): 136-142

[2] Ryu JS and Otsuki N. Crack closure of Reinforced Concrete by Electrodeposition Technique[J]. *Cement and Concrete Research*, 2002, 32(1): 159-164

[3] Ryu JS and Otsuki N. Experimental Study on Repair of Concrete Structural Members by Electrochemical Method[J]. *Scripta Materialia*, 2005, 52: 1 123-1 127

[4] Chu HQ and Jiang LH. Experimental Study on Electrodeposition Method for Repair of Concrete Cracks[J]. *Journal of Hohai University (Natural Sciences)*, 2005,33(3):310-313

[5] Jiang LH. *Concrete Material Science*[M]. Nanjing: Hohai University Press, 2006

[6] Li SL, Fan WG, Cai WC, *et al.* Laboratory tests of Electrochemical Removal of Chloride for Anti-corrosion[J]. *Hydro-Science And Engineering*, 2001, (3): 35-40

[7] Chen S. *The Deterioration Law and Service Life Prediction of Fly Ash Concrete under Coupling Effect of Load and Environment* [D]. Nanjing: Southeast University, 2008: 74-76